Head and Neck Pathology (2019) 13:286–297
https://doi.org/10.1007/s12105-018-0959-6

ORIGINAL PAPER

Identifying Candidate Biomarkers for Pleomorphic Adenoma: A Case–Control Study

Matthew D. Morrison[1] · Linda Jackson-Boeters[2] · Zia A. Khan[2] · Michael S. Shimizu[1] · Jason H. Franklin[3] · Kevin Fung[4] · John H. J. Yoo[4] · Mark R. Darling[5]

Received: 21 July 2018 / Accepted: 14 August 2018 / Published online: 17 August 2018

Abstract

Pleomorphic adenoma (PA) is the most common benign salivary gland tumor. Kallikrein-related peptidases have been identified as biomarkers in many human tumors and may influence tumor behavior. We investigated *KLK1−15* messenger ribonucleic acid and proteins in PA specimens to determine a KLK expression profile for this tumor. Fresh frozen PA tissue specimens ($n=26$) and matched controls were subjected to quantitative real-time reverse transcription polymerase chain reaction to detect *KLK1−15* mRNA. Expression of KLK1, KLK12, KLK13, and KLK8 proteins were then evaluated via immunostaining techniques. Statistical analyses were performed with the level of significance set at $P<.05$. We observed downregulation of *KLK1, KLK12*, and *KLK13* mRNA expression, and immunostaining studies revealed downregulation of the corresponding proteins. Histologic evidence of capsular perforation was associated with increased KLK1 protein expression. Tumor size was not associated with capsular invasion and/or perforation. This study is the first to detail a KLK expression profile for PA at both the transcriptional level and the protein level. Future work is required to develop clinical applications of these findings.

Keywords Pleomorphic adenoma · Salivary gland tumors · Kallikrein-related peptidases · Kallikreins · Immunohistochemistry · Biomarkers

Abbreviations

ACC	Acinic cell carcinoma
AdCC	Adenoid cystic carcinoma
ANOS	Adenocarcinoma not otherwise specified
AT_1	Angiotensin II receptor type 1
cDNA	Complementary deoxyribonucleic acid
C_T	Threshold cycle
DAB	3,3′-Diaminobenzidine
ECM	Extracellular matrix
EDTA	Ethylenediaminetetraacetic acid
ELISA	Enzyme-linked immunosorbent assay
FNA	Fine needle aspiration
HMGA2	High-mobility group AT-hook 2
IHC	Immunohistochemistry
IQR	Interquartile range
KKS	Kallikrein–kinin system
KLK	Kallikrein-related peptidase protein
KLK	Kallikrein-related peptidase gene
Mdn	Median
mRNA	Messenger ribonucleic acid
NSGT	Normal salivary gland tissue
OSS	Overall staining score

✉ Matthew D. Morrison
matthew.morrison@londonhospitals.ca

[1] Division of Oral and Maxillofacial Surgery, Department of Dentistry, London Health Sciences Centre, 339 Windermere Road, London, ON N6A 5A5, Canada

[2] Department of Pathology and Laboratory Medicine, University of Western Ontario, 1151 Richmond Street, London, ON N6A 5C1, Canada

[3] Division of Head and Neck Oncology and Reconstructive Surgery, Department of Otolaryngology, Kingston Health Sciences Centre, 144 Brock Street, Kingston, ON K7L 5G2, Canada

[4] Division of Head and Neck Oncology and Reconstructive Surgery, Department of Otolaryngology, London Health Sciences Centre, 339 Windermere Road, London, ON N6A 5A5, Canada

[5] Division of Oral and Maxillofacial Pathology, Department of Pathology and Laboratory Medicine, University of Western Ontario, 1151 Richmond Street, London, ON N6A 5C1, Canada

PA	Pleomorphic adenoma
PBS	Phosphate-buffered saline
PLAG1	Pleomorphic adenoma gene 1
PLGA	Polymorphous low-grade adenocarcinoma
RNA	Ribonucleic acid
RT-qPCR	Quantitative real-time reverse transcription polymerase chain reaction
SEM	Standard error of the mean
siRNA	Small interfering ribonucleic acid
SPINK6	Serine protease inhibitor of Kazal-type 6

Introduction

Pleomorphic adenoma (PA), also known as benign mixed tumor, is the most common salivary gland neoplasm in all age groups [1]. This tumor accounts for approximately 60–70% of all salivary gland neoplasms, is most common in adults between the ages of 30 and 60, has a slight female predilection, and has a high recurrence rate; however, with adequate surgery, a cure rate of more than 95% is achievable [2, 3]. PA arises in the parotid gland in about 80% of cases, particularly in the tail and inferior aspect of the gland; other locations include the submandibular gland (~ 10%), minor salivary glands (~ 10%), and the sublingual gland (0.3–1%). Surgical treatment of PA by superficial parotidectomy results in decreased recurrence rates compared to simple enucleation of the tumor [1]. Malignant transformation to carcinoma ex-pleomorphic adenoma occurs in 5–10% of cases, making carcinoma ex-PA the fourth most common malignant salivary gland tumor. Cytogenetic analysis has shown translocations in pleomorphic adenoma gene 1 (*PLAG1*) located at chromosome region 8q12 in approximately 70% of PAs [3]. Recurrent translocations involving the high-mobility group AT-hook 2 (*HMGA2*) gene are also present in a subset of PAs and carcinoma ex-PAs [4]. Finally, a variety of kallikrein-related peptidase genes (*KLKs*) have been linked to salivary gland tumors, including PA [5–7].

Kallikrein-1 (KLK1) and the remaining kallikrein-related peptidases (KLK2−15) are a family of 15 homologous secreted serine endopeptidases [5–7]. KLKs are involved in a wide range of normal physiological processes, such as skin desquamation, semen liquefaction, enamel formation, and regulation of the immune response [6, 8, 9]. Studies have also revealed that dysregulation of KLK expression, activity, or localization is frequently associated with pathological disorders, such as respiratory diseases, skin diseases, perturbation of tooth enamel formation, neurological disorders, and carcinogenesis [10–13]. KLKs control the growth of cancer cells by regulating the bioactivity of several hormones and growth factors through cell surface receptor activation [11]. Furthermore, KLKs promote cancer cell migration and invasion due to their proteolytic action on the extracellular matrix (ECM) [14]. Due to this functional role of KLKs in cancer progression, researchers have studied their utility as therapeutic targets [8, 15] and as biomarkers for disease [16–18].

KLKs may be exploited as biomarkers for tumor diagnosis and postoperative monitoring in the management of salivary gland neoplasms [19–21]. Salivary gland tumors comprise 0.5% of all malignancies and 2–5% of all head and neck malignancies worldwide [22–24]. Due to the relatively low incidence rates of salivary gland tumors, it is possible that the impact of these neoplasms is misrepresented. To date, the upregulation of KLKs in malignant tumors has been associated with both favorable and poor prognoses [25]. The potential for certain members of the KLK family to guide differential diagnoses, subtyping, and monitoring of patients with salivary gland tumors has been a driving force for research in this field.

The determination of a *KLK* mRNA and protein expression profile for PA may help to establish a link between KLK dysregulation and the pathophysiology of this tumor. Research groups have analyzed a variety of salivary gland neoplasms to determine relative KLK protein expression compared to normal salivary gland tissue (NSGT) controls [26–33]; such neoplasms include PA, adenoid cystic carcinoma (AdCC), acinic cell carcinoma (ACC), polymorphous low-grade adenocarcinoma (PLGA), mucoepidermoid carcinoma (MEC), and adenocarcinoma not otherwise specified (ANOS). In developing a KLK profile for PA, we hope to further our understanding of the roles of KLKs in PA tumorigenesis; furthermore, these findings may facilitate the development of clinical applications for guiding the differential diagnosis, prognosis, and postoperative monitoring of this salivary gland neoplasm.

The aims of this study were to (i) quantitate and compare the expression levels of *KLK1−15* mRNA in PA specimens and NSGT controls using quantitative real-time reverse transcription polymerase chain reaction (RT-qPCR); (ii) to analyze protein expression for dysregulated KLKs (determined in [i]) via immunostaining techniques; (iii) to identify associations between histologic evidence of capsular violation (i.e., invasion and/or perforation) and the expression of *KLK* mRNA and proteins in PA specimens; (iv) to identify associations between histologic evidence of capsular violation and PA tumor size; and (v) to investigate associations between KLK expression and PA recurrence and/or malignant transformation. This is the first report to characterize a KLK profile for PA at both the mRNA and protein level.

Methods

Approval for this case-control study was granted by the University of Western Ontario Health Sciences Research Ethics Board for research involving human subjects. Tissue

specimens were obtained from 26 ($n = 26$) subjects who underwent surgical treatment for PA between November, 2007, and December, 2008, at the Department of Otolaryngology-Head & Neck Surgery, London Health Sciences Centre, London, Ontario, Canada. Diagnosis of the lesion was based on criteria determined from the World Health Organization classification of tumors [34]. Normal salivary gland tissue lying outside the tumor capsule was also harvested from each site, which allowed each subject to serve as his/her own control. After surgical resection, both the PA specimens and control tissues were immediately snap-frozen in liquid nitrogen for storage in a freezer cooled to − 80 °C.

The sole selection criterion was confirmation of diagnosis (PA or NSGT) by histologic examination. Patient ages ranged from 19 to 84 years with a mean of 48 years, and the female-to-male ratio was approximately 2:1 (Table 1). Tumor specimens were retrieved from parotid gland (21 subjects, 81%) and submandibular gland (5 subjects, 19%) tissues. It should be noted that only 17 of the original 26 samples provided sufficient RNA yield for subsequent analyses. The modified age range for usable cases was 20–84 years with a mean of 53 years, and the female-to-male ratio was 11:6. Sixteen tumors were in parotid gland (16 subjects, 94%) and 1 tumor was in submandibular gland (1 subject, 6%) tissue.

RT-qPCR

Specimens were retrieved from the freezer and allowed to warm to room temperature (20−25 °C). A 100-mg piece of tissue was added to a 1.5-mL sterile centrifuge tube and combined with 1-mL of TRIzol Reagent (Thermo Fisher Scientific, Carlsbad, CA, USA, Catalog number: 15596026) for RNA isolation. The solution was homogenized using a homogenizer. The lysate was centrifuged (12,000×*g*) for 5 min at 4–10 °C, then the supernatant was transferred to a new tube. The solution was incubated for 5 min to permit complete dissociation of the nucleoproteins complex. Next, 0.2 mL of chloroform was added to the tube and the tube cap was closed. This solution was incubated for 2–3 min. The sample was then centrifuged (12,000×*g*) for 15 min at 4 °C. The mixture separated into three layers: a lower red phenol–chloroform phase, an interphase, and a colorless upper aqueous phase. The upper aqueous phase containing the RNA was transferred to a new tube using a pipette. A solution of 70% ethanol was combined in a centrifuge tube with the RNA solution in a 1:1 ratio (400-µL of each solution was used). The mixture was then hand-mixed. The Aurum Total RNA mini kit (Bio-Rad Laboratories, Hercules, CA, USA, Catalog number: 7326820) was next assembled and utilized according to protocol. Measurements of RNA quantities were then performed using the Qubit RNA BR Assay Kit (Thermo Fisher Scientific, Carlsbad, CA, USA, Catalog number: Q10210).

Subsequent experiments involved reverse transcription of isolated RNA into complementary DNA (cDNA) using the iScript cDNA Synthesis Kit (Bio-Rad Laboratories, Hercules, CA, USA, Catalog number: 1708890). Next, RT-qPCR reactions were carried out using the CFX Connect Real-Time PCR Detection System (Bio-Rad Laboratories, Hercules, CA, USA). Each custom PCR plate accommodated six specimens and came loaded with *KLK*1−15 and β-actin primer assays from the supplier (Qiagen, Germantown, MD, USA). Polymerase chain reaction mixtures consisted of the following: 10-µL of SsoFast EvaGreen Supermix (Bio-Rad Laboratories, Hercules, CA, USA, Catalog number: 1725201), 2-µL of primer assay (*KLK* + β-actin), 1-µL of previously synthesized *KLK* cDNA, and 7-µL of nuclease-free water. It should be noted that the SsoFast EvaGreen Supermix contained dNTPs, magnesium chloride, Sso7d-fusion polymerase, EvaGreen dye and stabilizers. A 20-µL volume of the reaction mixture was transferred by pipette to the appropriate well on a PCR plate. The RT-qPCR protocol involved one cycle of 10 min at 95 °C for enzyme activation, followed by 40 cycles of 15 s at 95 °C for denaturation and 40 cycles of 1 min at 60 °C for annealing/extension. The specificity of each PCR amplification was verified by post-RT-qPCR melting curve analysis.

Relative quantitation of RT-qPCR data was performed using the comparative C_T ($\Delta\Delta C_T$) method. The threshold cycle (C_T) of each *KLK* (i.e., *KLK1−15*) in PA or control specimens was normalized to the corresponding C_T of the housekeeping gene, β-actin, to yield a ΔC_T value. Subsequent calculations for mean ΔC_T, standard deviation, $\Delta\Delta C_T$, mean $\Delta\Delta C_T$, and standard error of the mean (SEM) values were performed using GraphPad Prism, Version 7.0c for Mac OS X (GraphPad Software, CA, USA). The paired ΔC_T values were subjected to Wilcoxon signed-rank test with the level of significance set at $P < .05$.

Table 1 Demographic characteristics of the study population

	All specimens		Usable specimens[a]	
n	26		17	
Age range (years)	19–84		20–84	
Gender	Female	Male	Female	Male
	17	9	11	6
Tumor location	PG	SMG	PG	SMG
	21	5	16	1

PG parotid gland, *SMG* submandibular gland, *RNA* ribonucleic acid

[a]Sufficient RNA yield for subsequent analyses

Immunohistochemistry

For immunohistochemistry (IHC) experiments, each of the 26 PA specimens and matched NSGTs were fixed in formalin and embedded in paraffin to facilitate histologic slide preparation according to known techniques [35]. The antibodies used in this study were chosen based on the results of our RT-qPCR analyses. For PA specimens having KLK ΔC_T values that were significantly greater or lesser than the values for matched control tissues, the corresponding KLK antibodies were used: KLK1 (Bioss, MA, USA, Catalog number: BS-1963R), KLK12 (Novus Biologicals, CO, USA, Catalog number: NB200-137), KLK13 (Abcam, ON, Canada, Catalog number: AB113227), and KLK8 (Abgent, CA, USA, Catalog number: genta-AP6327B). While the ΔC_T value for *KLK8* in all PA samples was not significantly different from ΔC_T value for control tissues, the KLK8 antibody was used as a reference in the immunostaining experiments.

Evaluation of KLK1, KLK12, KLK13, and KLK8 expression in PA and matched NSGT specimens was performed using standard immunostaining techniques. Positive control tissues (i.e., skin or prostate gland) known to express each respective KLK were used to demonstrate a positive staining reaction and to guide preparation of KLK antibody titers [17, 19, 30, 36–40]. IHC procedures performed on tissues with primary antibody omitted served as negative controls. Both the negative and positive controls were batch controls, not "on-slide" controls. Using the calculated dilution of 1/1000 for the KLK1 polyclonal antibody, PA and NSGT specimens were subjected to the immunostaining protocol. The calculated dilutions of 1/100, 1/2000, and 1/200 were used for the KLK12, KLK13, and KLK8 polyclonal antibodies, respectively. It should be noted that PA specimens used for immunostaining did not show a statistically significant alteration in KLK8 expression relative to NSGT. The intention was to compare staining immunoreactivity scores for the dysregulated KLKs (*i.e.*, KLK1, KLK12, and KLK13) with those for a non-dysregulated KLK (i.e., KLK8).

To prepare the slides for immunostaining, they were first deparaffinized then hydrated through xylenes and a graded ethanol series. The following protocol was then followed for the KLK1, KLK12, KLK13, and KLK8 experiments:

Antigen retrieval was performed using citrate buffer (at pH 6.0) in a decloaking chamber at 125 °C for the KLK12 and KLK13 antigens; for the KLK1 and KLK8 antigens, ethylenediaminetetraacetic acid (EDTA) buffer (at pH 9.0) was used. After antigen retrieval, slides were rinsed and blocked using 10% horse serum. Incubation with the KLK-specific primary antibody was performed using the appropriate dilution, temperature, and time frame. After allowing antibodies to bind antigens overnight, excess antibody was removed by rinsing with phosphate-buffered saline (PBS). Slides were then treated with the secondary antibody (ImmPRESSTM HRP Anti-Rabbit IgG [Peroxidase] Polymer Detection Kit, Vector Laboratories, CA, USA, Catalog number: MP-7401) and incubated at room temperature for 30 min. After rinsing with PBS, a 3,3′-diaminobenzidine (DAB) solution (Vector Laboratories, CA, USA, Catalog number: SK-4100) was applied to the slides for 6–8 min. Deactivation of the DAB solution was achieved by rinsing the slides with water for 5 min. Counterstaining was performed with haematoxylin. Dehydration was achieved by transferring slides through a graded ethanol series followed by a soak in xylenes. Coverslips were applied to the slides using Cytoseal Mounting Medium (VWR, ON, Canada, Catalog number: 48212154). Immunostaining in PA and NSGT specimens is shown for KLK1 (Fig. 1a, b), KLK12 (Fig. 1c, d), KLK13 (Fig. 2a, b), and KLK8 (Fig. 2c, d).

A semi-quantitative analysis of the immunostained slides was performed under light microscopy according to previously described techniques [31, 32]. The proportion score represented the estimated fraction of positively staining tumor cells (where 0 = none; 1 < 1/100; 2 = (1/100)–(1/10); 3 = (1/10)–(1/ 3); 4 = (1/3)–(2/3); and 5 > 2/3). For staining intensity, the score was represented by the estimated average intensity of staining for tumor cells (where 0 = none; 1 = weak; 2 = intermediate; and 3 = strong). The overall amount of positive staining was then expressed as the sum of the proportion and intensity scores, known as the Overall Staining Score (OSS; ranges: 0 for negative staining, and 2–8 for positive staining). In tumor tissue, cells lining duct-like structures and non-ductal cells were scored for extent of positive staining and staining intensity. For the purposes of this study, duct-like cells were regarded as cells that lined the lumina of duct-like structures within tumor tissues, while non-ductal cells were any tumor cells that were not obviously lining ducts. The staining was assessed by two trained examiners, with comparison and correlation of assessments to produce consistency and to reduce inter-examiner variability. Statistical calculations were performed using GraphPad Prism, Version 7.0c for Mac OS X (GraphPad Software, CA, USA). The level of significance was set at $P < .05$. Dot plots were prepared to display OSS values for each KLK-specific antibody (Figs. 3, 4, 5, 6).

Assessment of Capsular Invasion and/or Perforation

To assess the capsular violation phenomena in tumor tissues, the original histology slides used for diagnosing PA in cases 1–26 were analyzed for evidence of capsular invasion and/or perforation. Capsular invasion was defined as penetration of PA tumor cells into—but not completely through—the fibrous tumor capsule. Capsular perforation was defined as penetration of PA tumor cells completely through the fibrous tumor capsule into the surrounding normal tissues. Representative slides were chosen to demonstrate each type

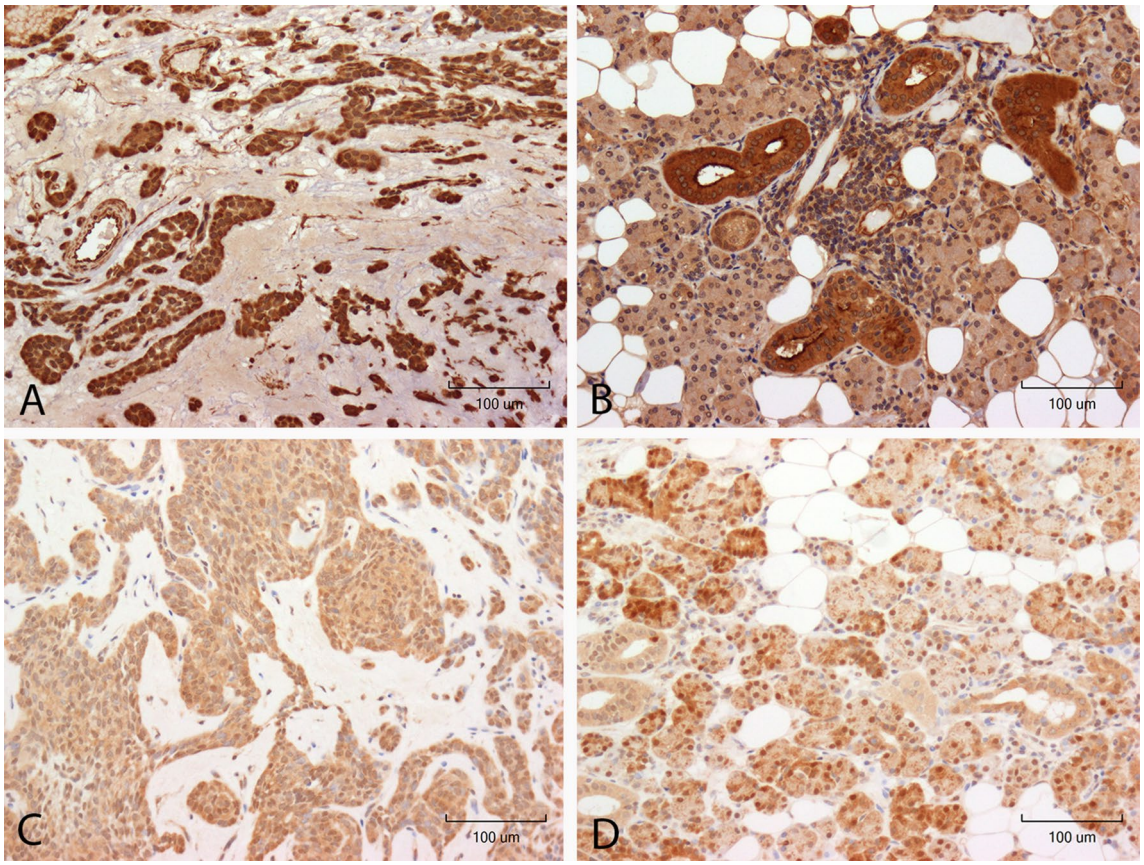

Fig. 1 Immunostaining for KLK1 (brown staining in cytoplasm of cells) in representative PA (**a**) and NSGT (**b**) specimens (original magnification ×200); Immunostaining for KLK12 (brown staining in cytoplasm of cells) in representative PA (**c**) and NSGT (**d**) specimens (original magnification ×200). *PA* pleomorphic adenoma, *NSGT* normal salivary gland tissue, *KLK* kallikrein

of capsular violation (Fig. 7a–d). A thick, intact capsule was found for the PA in Fig. 7a. Invasion of tumor into the fibrous capsule was shown for the PA in Fig. 7b. Perforation of tumor through the capsule was identified for the PA in Fig. 7c. Lastly, a positive tumor margin was shown for the PA in Fig. 7d. Statistical analysis was performed to determine associations between capsular violation (i.e., invasion and/or perforation) and *KLK* mRNA and/or proteins. Statistical calculations were carried out using GraphPad Prism, Version 7.0c for Mac OS X (GraphPad Software, CA, USA) and the level of significance was set at $P < .05$. A Mann–Whitney *U* test was performed to compare mean mRNA values (based on $\Delta\Delta C_T$ calculations) for *KLK1, KLK12*, and *KLK13* in the various PA cases (Table 2). Likewise, a Mann–Whitney *U* test was employed for comparison of the OSS values for ductal cells and non-ductal cells in the various PA cases showing capsular violation (Table 3).

Tumor Size

Surgical pathology reports for cases 1–26 were examined to obtain measurements of gross tumor specimens such that associations with capsular violation could be determined (Table 4). The level of significance for all statistical tests was set at $P < .05$.

Results

RT-qPCR

From the original 26 paired PA and NSGT specimens, only 17 pairs (65%) produced sufficient RNA yield for cDNA synthesis and subsequent RT-qPCR analyses (see Table 1). All 17 pairs of samples were analyzed and the corresponding ΔC_T values for each *KLK* were recorded. Our RT-qPCR experiments revealed a statistically significant decrease in mRNA expression for *KLK1* ($P = .0114$), *KLK12* ($P = .0444$), and *KLK13* ($P = .0278$) in PA relative to NSGTs. In contrast, there were no statistically significant differences in *KLK2−11, KLK14*, and *KLK15* expression between PA and NSGT specimens ($P > .05$).

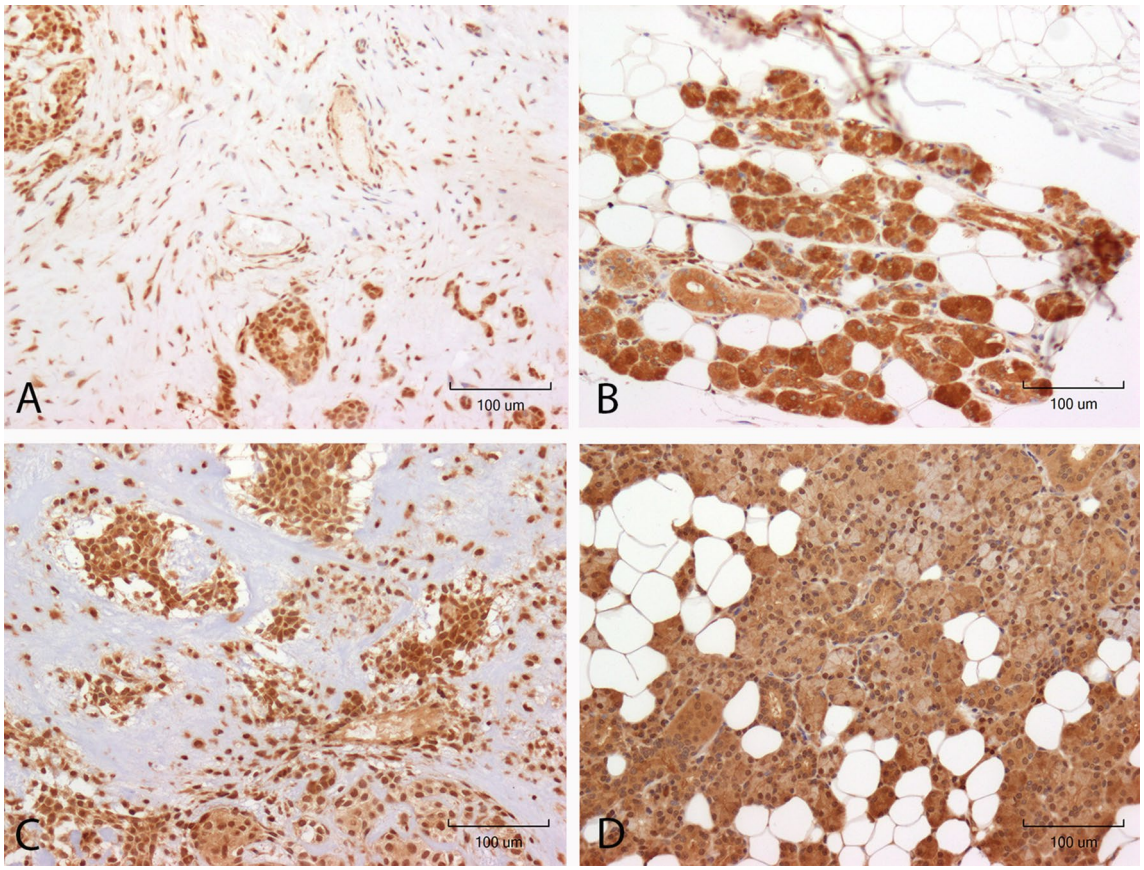

Fig. 2 Immunostaining for KLK13 (brown staining in cytoplasm of cells) in representative PA (**a**) and NSGT (**b**) specimens (original magnification ×200); immunostaining for KLK8 (brown staining in cytoplasm of cells) in representative PA (**c**) and NSGT (**d**) specimens (original magnification ×200). *PA* pleomorphic adenoma, *NSGT* normal salivary gland tissue, *KLK* kallikrein

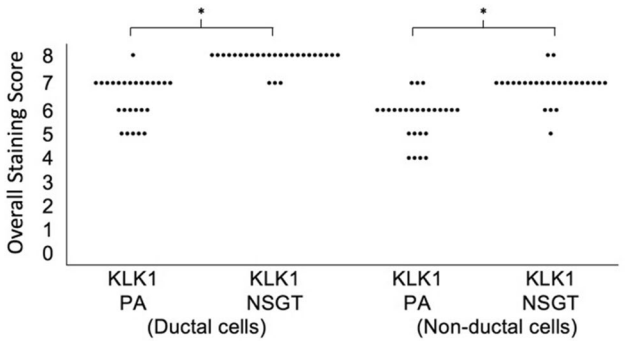

Fig. 3 OSS values for KLK1 in ductal cells and non-ductal cells of PA and NSGT specimens. *OSS* overall staining score, *KLK* kallikrein, *PA* pleomorphic adenoma, *NSGT* normal salivary gland tissue. *$P < .0001$

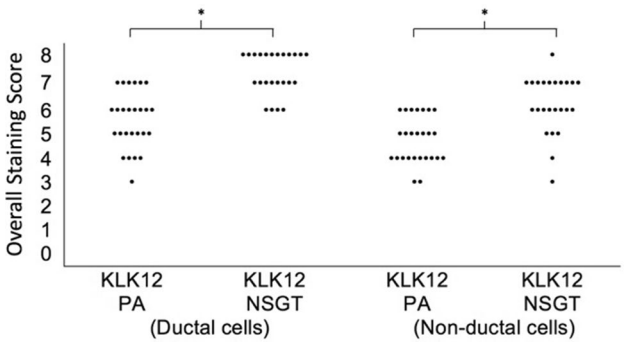

Fig. 4 OSS values for KLK12 in ductal cells and non-ductal cells of PA and NSGT specimens. *OSS* overall staining score, *KLK* kallikrein, *PA* pleomorphic adenoma, *NSGT* normal salivary gland tissue. *$P < .0001$

Immunohistochemistry

Staining immunoreactivity scores (i.e., OSS) were calculated for all PA and NSGT specimens treated with KLK1, KLK12, KLK13, or KLK8 polyclonal antibodies (see Figs. 1, 2). Table 2 demonstrates a statistically significant decrease in OSS values for KLK1 in ductal cells with 7.0 and 8.0 for PA and NSGT, respectively [*P* (ductal cells) < .0001]. There was also a statistically significant decrease in OSS values for KLK1 in non-ductal cells with 6.0 and 7.0 for PA and NSGT, respectively [*P* (non-ductal

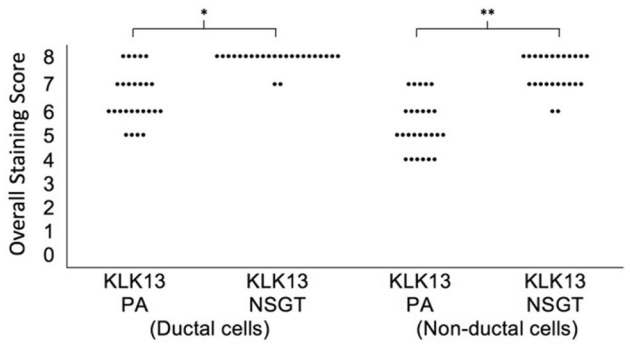

Fig. 5 OSS values for KLK13 in ductal cells and non-ductal cells of PA and NSGT specimens. *OSS* overall staining score, *KLK* kallikrein, *PA* pleomorphic adenoma, *NSGT* normal salivary gland tissue. *$P = .0001$, **$P < .0001$

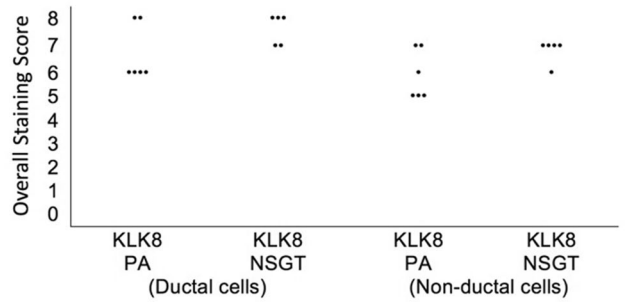

Fig. 6 OSS values for KLK8 in ductal cells and non-ductal cells of PA and NSGT specimens. *OSS* overall staining score; *KLK* kallikrein, *PA* pleomorphic adenoma, *NSGT* normal salivary gland tissue

cells) < .0001]. The corresponding values for KLK12 in ductal cells were 5.5 and 7.0 for PA and NSGT, respectively [*P* (ductal cells) < .0001], and 4.0 and 6.0 for PA and NSGT, respectively, in non-ductal cells [*P* (non-ductal cells) < .0001]. The corresponding values for KLK13 in ductal cells were 6.0 and 8.0 for PA and NSGT, respectively [*P* (ductal cells) = .0001], and 5.0 and 7.5 for PA and NSGT, respectively, in non-ductal cells [*P* (non-ductal cells) < .0001] (Table 2; Figs. 3, 4, 5). No statistically significant differences were observed for KLK8 immunostaining [*P* (ductal cells) = .1250, *P* (non-ductal cells) = .1250] in PA and NSGT specimens (Table 2; Fig. 6). Based on the immunostaining analyses, it was evident that median OSS values for PA specimens were greater in ductal cells than in non-ductal cells, which was consistent with previous observations in the literature [26, 28, 31]. No stromal staining was observed for any of the PA specimens. Overall, the statistically significant, albeit small, differences in OSS values for the dysregulated KLKs in PA and NSGT specimens support the findings established at the mRNA level.

Capsular Invasion and/or Perforation

There were no statistically significant differences in the mRNA levels of *KLK1* (*P* = .2345), *KLK12* (*P* = .0830), and *KLK13* (*P* = .5737) in PA specimens with different capsular violation phenomena (i.e., invasion and/or perforation) (Table 3). There were also no statistically significant differences in median OSS values for KLK12 [*P* (ductal cells) = .3170, *P* (non-ductal cells) = .4094] and KLK13 [*P* (ductal cells) = .9159, *P* (non-ductal cells) = .5961] proteins in PA specimens (Table 4), but there was a statistically significant increase in the median OSS values for KLK1 in cases with capsular perforation [*P* (ductal cells) = .0135, *P* (non-ductal cells) = .0470].

Tumor Size

Our investigations demonstrated no statistically significant differences in tumor size between PAs with capsular invasion and/or perforation (*P* > .05; Table 5).

Recurrence and/or Malignant Transformation

Review of the medical records for each subject was performed to determine the number of cases with tumor recurrence and/or malignant transformation. At the 10-year follow-up mark, none of the 26 PA cases had a documented tumor recurrence or malignant transformation. Only one case had a positive tumor margin (see Fig. 7d), but this case did not present with a recurrence or malignant transformation during the follow-up period. It should be noted that 3 of the 26 cases had died due to unrelated causes during the 10-year postoperative period.

Discussion

To date, our study is the first to identify statistically significant downregulation of *KLK1, KLK12*, and *KLK13* mRNA and proteins in PA specimens. Considering the variety of diseases involving up- and downregulation of KLKs, our findings suggest the involvement of a KLK cascade in the pathophysiology of PA; specifically, the downregulated expression levels of KLK1, KLK12, and KLK13 in PA may account for the low incidence of capsular invasion and/or malignant transformation. The observed downregulation may involve one or more KLK inhibitors, such as SPINK6, which has been shown to inhibit KLK12 and KLK13, but not KLK1 [41]; however, future work is required to identify such phenomena.

The non-invasive, benign nature of PA could in part be explained by downregulation of KLK1, which is necessary for tumor cell migration, vascular sprouting, and

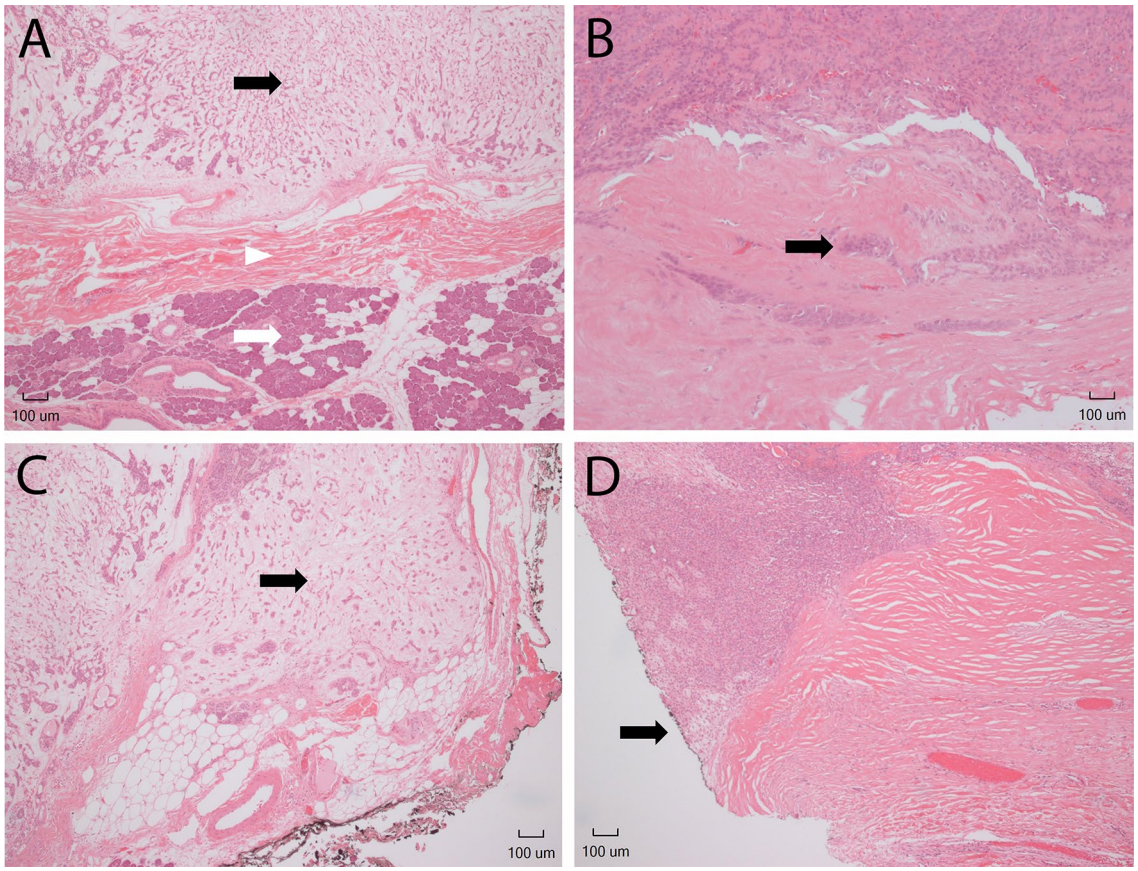

Fig. 7 Haematoxylin-eosin stains showing PA (black arrow), intact fibrous capsule (white triangle) and NSGT (white arrow) (**a**); invasion of pleomorphic adenoma (black arrow) into fibrous capsule (**b**); perforation of pleomorphic adenoma (black arrow) through fibrous capsule (**c**); and positive PA resection margins (black arrow) (**d**) (original magnification ×50). *PA* pleomorphic adenoma, *NSGT* normal salivary gland tissue

Table 2 Calculated OSS values for dysregulated KLK proteins in ductal and non-ductal cells of PA specimens

	Ductal cells				Non-ductal cells			
	n	Mdn OSS	IQR	*P*-value	*n*	Mdn OSS	IQR	*P*-value
KLK1								
PA	26	7.0	6.0–7.0	< .0001*	26	6.0	5.0–6.0	< .0001*
NSGT	26	8.0	8.0–8.0		26	7.0	7.0–8.0	
KLK12								
PA	24	5.5	5.0–6.0	< .0001*	24	4.0	4.0–5.0	< .0001*
NSGT	24	7.0	7.0–8.0		24	6.0	5.3-7.0	
KLK13								
PA	24	6.0	6.0–7.0	.0001*	24	5.0	5.0–6.0	< .0001*
NSGT	24	8.0	8.0–8.0		24	7.5	7.0–8.0	
KLK8								
PA	5	6.0	6.0–7.0	.1250	5	5.0	5.0–6.5	.1250
NSGT	5	8.0	7.0–8.0		5	7.0	6.5–7.0	

PA pleomorphic adenoma, *NSGT* normal salivary gland tissue, *Mdn* median, *OSS* overall staining score, *IQR* interquartile range

*$P < .05$

Table 3 Association between dysregulated *KLK* mRNA and capsular violation phenomena in PA specimens

	Capsular violation	Mean mRNA level (SEM)	*P*-value
KLK1	Invasion ($n=8$)	8.528 (1.550)	.2345
	Perforation ($n=8$)	0.071 (5.499)	
KLK12	Invasion ($n=8$)	13.570 (0.828)	.0830
	Perforation ($n=8$)	11.290 (0.651)	
KLK13	Invasion ($n=8$)	10.050 (5.408)	.5737
	Perforation ($n=8$)	9.411 (5.191)	

KLK kallikrein, *mRNA* messenger ribonucleic acid, *PA* pleomorphic adenoma

Table 4 Association between OSS values and capsular violation phenomena for dysregulated KLK proteins in ductal and non-ductal cells of PA specimens

	Capsular violation	Mdn OSS (IQR)	*P*-value
Ductal cells			
KLK1	Invasion ($n=11$)	6.0 (6.0–7.0)	.0135
	Perforation ($n=14$)	7.0 (7.0–7.0)	
KLK12	Invasion ($n=9$)	5.0 (4.5–6.0)	.3170
	Perforation ($n=14$)	6.0 (4.8–7.0)	
KLK13	Invasion ($n=9$)	6.0 (5.5–7.5)	.9159
	Perforation ($n=14$)	6.0 (6.0–7.0)	
Non-ductal cells			
KLK1	Invasion ($n=11$)	6.0 (5.0–6.0)	.0470
	Perforation ($n=14$)	6.0 (6.0–6.3)	
KLK12	Invasion ($n=9$)	4.0 (4.0–5.5)	.4094
	Perforation ($n=14$)	5.0 (4.0–6.0)	
KLK13	Invasion ($n=9$)	5.0 (4.5–6.5)	.5961
	Perforation ($n=14$)	5.5 (5.0–6.3)	

OSS overall staining score, *KLK* kallikrein, *PA* pleomorphic adenoma, *Mdn* median, *IQR* interquartile range

Table 5 Association between specimen size and capsular violation phenomena in PA specimens

Capsular violation	Mean size (cm^3)	SEM (cm^3)	*P*-value
Invasion ($n=11$)	7.800	5.065	.3238
Perforation ($n=13$)	4.252	0.960	

PA pleomorphic adenoma, *SEM* standard error of the mean

angiogenesis. In normal physiology, KLK1 is most abundantly produced in the pancreas and salivary glands, followed by the colon and the small intestine [36, 38, 40]; lower concentrations are found in esophagus, kidney, lymph node, prostate, stomach, thyroid, ureter, and vaginal tissues [36]. KLK1 is a key player in the tissue kallikrein-kinin system (KKS)—a system regarded as one of the main mechanisms controlling systemic and local hemodynamics [42]. Studies have implicated this system in the protection from hypertension, vascular remodeling, and renal fibrosis [42, 43]. Kallikrein-1 is constitutively expressed by endothelial cells and it is released upon endothelial cell activation to digest the vascular basement membrane and interstitial matrix [44, 45]. These processes are necessary for migration, vascular sprouting, and angiogenesis. In the presence of decreased KLK1 levels, there may be a reduced rate of vascular basement membrane and interstitial matrix digestion, resulting in slower tumor growth.

Decreased *KLK12* mRNA and protein expression have been shown to inhibit tumor cell proliferation in AGS gastric cancer cells [46], and similar processes may occur in PA. KLK12 is highly expressed in a variety of endocrine tissues, including salivary gland and stomach, and dysregulation at the gene and protein levels has been linked to tumorigenesis [36, 46]. One group of investigators evaluated the effects of *KLK12* mRNA and protein downregulation on the cell cycle and proliferation of AGS cells—a human gastric adenocarcinoma cell line [46]. The observed *KLK12* mRNA and protein expression levels were higher in AGS cells than the GES-1 normal gastric epithelial cells. Transfection of AGS cells with KLK12 small interfering RNA (siRNA) led to downregulation of *KLK12* mRNA and protein expression, reduced cell proliferation, and lower cell counts with respect to the negative control. *KLK12* siRNA increased the number of AGS cells in G0/G1 and reduced those in S phase of the cell cycle. Moreover, downregulation of *KLK12* in AGS cells decreased their ability to penetrate the membrane in a migration assay. Overall, *KLK12* siRNA inhibited the proliferation and migration of AGS gastric cancer cells and caused their arrest in the G0/G1 phase of the cell cycle. Similarly, the downregulation of KLK12 in PA may account for the relatively slow rate of tumor growth.

Multiple KLK inhibitors have thus been shown to independently regulate KLK activity and these findings may help to explain the observed downregulation of *KLK12* and *KLK13* mRNA and proteins in PA. The known sequestration of KLKs by serum protease inhibitors prompted researchers to investigate the interaction of KLK13 with similar inhibitors [47]. Recombinant KLK13 produced in yeast was added to male and female sera and various biological fluids, and the samples were analyzed with a KLK13 enzyme-linked immunosorbent assay (ELISA). Enzymatically active KLK13 was labelled with I-125 and used for in vitro reactions with candidate protease inhibitors and serum samples. The identified inhibitors included α2-antiplasmin, α2-macroglobulin, and α1-antichymotrypsin. Another research group revealed that members of the SPINK family regulate KLK activity through inhibition [48]. These investigators found that SPINK6 exhibited inhibitory activity against KLK12 and KLK13, but not against KLK1, KLK3, and KLK11. Overall, these findings suggest a mechanism for KLK inhibition

which could affect KLK expression in PA, but further studies are required to elucidate such processes.

KLK13 cleaves the major components of ECM and is believed to be involved in tissue remodeling, and/or tumor invasion and metastasis [49, 50], which prompted studies of its role in the pathogenesis of salivary gland tumors [30]. A research group recently analyzed the expression levels of KLK13 in benign and malignant salivary gland tumors [31]. Using immunostaining analyses, normal tissues were compared to samples from PA, AdCC, PLGA, ACC, MEC, and ANOS. The results indicated that KLK13 expression was upregulated in most salivary gland tumors. Immunostaining for KLK13 in PA was significantly reduced relative to control samples. Conversely, immunostaining for KLK13 in PLGA, AdCC, and ANOS was significantly increased relative to controls. MEC and ACC did not display much deviation in staining immunoreactivity compared to healthy tissues. When ductal structures were assessed, ductal cells and cells lining duct-like structures revealed more prominent immunostaining intensity than non-ductal cells in most tumors. Overall, these investigators were the first to report downregulation of KLK13 in PA. Our study corroborated these findings for PA and additionally revealed downregulation of *KLK13* mRNA compared to control tissues. Such alterations in KLK13 mRNA and proteins may account for the slow rate of growth and benign nature of PA. Downregulation of KLKs in PA may also decrease the invasion and/or perforation of tumor cells through the fibrous capsule.

Rather than digestion of capsular tissues by KLKs, a more plausible explanation for capsular violation phenomena in PA may be capsular rupture during preoperative fine needle aspiration (FNA) biopsy [51]. This phenomenon, known as capsular pseudoinvasion, has been documented after FNA of follicular adenomas of the thyroid [52]. The lack of differences in mRNA levels for *KLK1, KLK12*, and *KLK13* in PA cases showing capsular invasion and/or perforation supported the assumption that *KLKs* are not directly responsible for such histological findings. This was reinforced by the decreased expression of KLK12 and KLK13 proteins; however, the increased expression of KLK1 proteins in cases with capsular perforation contradicted this assumption. Overall, it appears that KLK proteins are not involved in the digestion of capsular tissues to produce capsular invasion and/or perforation, but follow-up experiments are required to clarify such associations.

Consideration of the various PA specimen sizes prompted us to investigate correlations between tumor size and the presence or absence of capsular violation. Since PA may grow to massive proportions over decades, we surmised that larger tumors would not be more likely to demonstrate violation of the fibrous capsule. We observed no significant differences in PA specimen sizes between cases demonstrating capsular invasion and/or perforation, which supported the likelihood that capsular violation phenomena were not caused by digestion of capsular tissues by KLKs. The presence of an intact fibrous capsule allows PA not only to grow as a benign entity for many years, but also facilitates clean surgical dissection around the tumor, which reduces recurrence rates.

There was no documented case of tumor recurrence and/or malignant transformation for any of the study subjects at the 10-year follow-up mark. This finding was consistent with the decreased recurrence rates for modern surgical treatment of PA (i.e., partial superficial parotidectomy/complete submandibular gland excision vs. simple enucleation) and the low incidence of malignant transformation of this tumor [1].

Limitations and Future Work

Although it was not the intention of this study to offer final and conclusive solutions, the determination of a KLK profile for PA may help to establish a causative link between KLK dysregulation and the pathophysiology of this tumor. Our case-control study, while restricted by the small number of samples, is foundational work, which warrants further basic mechanistic studies and a large, multi-centered prospective trial.

The nature of the control tissues used were a limitation in this study. Analyzing matched NSGTs from PA-containing glands (i.e., parotid gland or submandibular gland) may have produced *KLK* mRNA and protein profiles which did not reflect those of healthy salivary gland tissues. Local and systemic host factors that may have contributed to the formation of PA may also have altered the *KLK* mRNA and protein expression in NSGTs. Moving forward, tissues from healthy salivary glands (e.g., contralateral glands, or glands from healthy controls) should be compared to PA specimens.

The specificity of our IHC staining and the strength of our OSS method were limited by the polyclonal nature of our KLK antibodies and the lack of blinding in the scoring process, respectively. Regarding the KLK-specific primary antibodies, a greater staining specificity may be obtained by using monoclonal antibodies; however, our options were limited to polyclonal antibodies due to the sparse availability of monoclonal antibodies for KLK1, KLK12, KLK13, and KLK8. The OSS method did not involve blinding of the observers to the tissues being examined, which may have introduced observer bias. It should also be noted that the small portions of PA and NSGTs provided by the surgical team did not allow for the preparation of enough histology slides to repeat our IHC experiments. In future studies, monoclonal KLK antibodies should be employed for greater staining specificity, the scoring of immunostaining should be a blinded process, and all immunostaining experiments should be repeated.

Alternatively, immunofluorescence reactions may be performed to allow for automatic quantification of KLK proteins, which would eliminate observer bias.

Future work may involve the development of a PA cell line, which could be utilized for KLK-specific analyses. Assessment of PA cells subjected to adenoviral delivery of *KLK1, KLK12*, and *KLK13* genes may strengthen the findings of this study if transfected cells demonstrated an increased incidence of invasion and/or malignant transformation. Moreover, identification of KLK1, KLK12, and KLK13 inhibitors in PA may help to explain the observed downregulation of these KLKs. Once KLK expression profiles for other salivary gland neoplasms including MEC, PLGA, AdCC, ACC, ANOS, and carcinoma ex-PA have been determined, a comparison of KLKs in PA and the malignant tumors may be made. If the malignant tumors demonstrated increased levels of KLK1, KLK12, and/or KLK13, it would be interesting to see if the delivery of nanoliposomes containing *KLK1-, KLK12*-, and *KLK13*-targeting siRNA would reduce tumor aggressiveness.

In addition to our current study, which analyzed KLK expression in PAs of major salivary glands, we plan to examine KLK expression in PAs of minor salivary gland origin. In doing so, we may develop a better understanding of KLK dysregulation in PAs, and capsular violation phenomena may be more critically examined due to incomplete capsule formation for PAs of minor salivary glands. One limitation for such a study would be the difficulty in collecting sufficient samples of PAs of minor salivary glands, which occur with much lower frequency than PAs of major salivary glands.

Other investigations may involve the development of multiparametric panels of KLK biomarkers for guiding the differential diagnosis, prognosis, and postoperative monitoring of PA. Gene regions to be investigated by targeted gene sequencing assays may include *PLAG1, HMGA2, KLK1, KLK12*, and *KLK13*. The additional information gleaned from KLK-specific IHC staining of FNA samples may improve diagnostic accuracy, which could greatly change the proposed management (e.g., simple enucleation for a benign tumor versus wide local excision for a malignant tumor). This combination of gene level and protein level analyses may facilitate more accurate differential diagnosis of salivary gland tumors, as previous studies have shown pitfalls in relying on immunohistochemistry alone [53]. To rule out distant metastases, serum levels of KLKs should also be investigated in conjunction with a comprehensive physical examination and review of systems. While the development of a simple and convenient serum or saliva test may not be possible for PA due to the downregulation of KLK proteins in this tumor, our foundational work may help to develop such tests for other salivary gland tumors.

Conclusions

To date, our study is the first to identify statistically significant downregulation of *KLK1, KLK12*, and *KLK13* mRNA and proteins in PA by RT-qPCR and IHC analyses, respectively. For PA cases with capsular perforation and invasion, we identified no statistically significant differences in *KLK1, KLK12*, or *KLK13* mRNA expression; however, a statistically significant increase in KLK1 protein was observed in ductal and non-ductal cells of PAs with capsular perforation. We found no significant differences in tumor size for PA cases with capsular violation (i.e., invasion and/or perforation). In the 10-year postoperative period, no PA cases showed any recurrence or malignant transformation. Given the variety of diseases involving up- and downregulation of KLKs, our findings suggest the involvement of a KLK cascade in the pathophysiology of PA; specifically, the decreased expression of *KLK1, KLK12*, and *KLK13* mRNA and proteins in PA may account for the low incidence of capsular invasion and/or malignant transformation. This foundational work may facilitate the development of clinical applications for KLKs in guiding the differential diagnosis, prognosis, and postoperative monitoring of PA.

Funding Funding was obtained from the University of Western Ontario (Dr. Mark R. Darling) and the Canadian Association of Oral and Maxillofacial Surgeons (Dr. Matthew D. Morrison).

Compliance with Ethical Standards

Conflict of interest There are no conflict of interest to disclose.

Ethical Approval All procedures performed in this study were in accordance with the ethical standards of the institutional and national research committee and with the 1964 Helsinki declaration and its later amendments or comparable ethical standards.

Informed Consent Informed consent was obtained from all individual participants included in the study.

References

1. Spiro RH. Salivary neoplasms: overview of a 35-year experience with 2,807 patients. Head Neck Surg. 1986;8:177–84.
2. Hellquist H, Skalova A. Histopathology of salivary glands. Berlin: Springer; 2014.
3. Neville BW, Damm DD, Allen CM, Bouquot JE, editors. Oral and maxillofacial pathology. 3rd ed. St. Louis: WB Saunders; 2009.
4. Mito JK, Jo VY, Chiosea SI, et al. HMGA2 is a specific immunohistochemical marker for pleomorphic adenoma and carcinoma ex-pleomorphic adenoma. Histopathology 2017;71(4):511–21.
5. Yousef GM, Diamandis EP. The expanded human kallikrein gene family: locus characterization and molecular cloning of a new member, KLK-L3 (KLK9). Genomics 2000;65(2):184–94.

6. Clements J, et al. The expanded human kallikrein (KLK) gene family: genomic organisation, tissue-specific expression and potential functions. Biol Chem. 2001;382(1):5–14.
7. Harvey TJ, et al. Tissue specific expression patterns and fine mapping of the human kallikrein (KLK) locus on proximal 19q13.4. J Biol Chem. 2000;275(48):37397–406.
8. Clements JA, et al. The tissue kallikrein family of serine proteases: functional roles in human disease and potential as clinical biomarkers. Crit Rev Clin Lab Sci. 2004;41(3):265–312.
9. Prassas L, et al. Unleashing the therapeutic potential of human kallikrein-related serine proteases. Nat Rev Drug Discov. 2015;14(3):183–202.
10. Bartlett JD, Simmer JP. Kallikrein-related peptidase-4 (KLK4): role in enamel formation and revelations from ablated mice. Front Physiol. 2014;5:240.
11. Batra J, et al. Genetic polymorphisms in the human tissue kallikrein (KLK) locus and their implication in various malignant and non-malignant diseases. Biol Chem. 2012;393(12):1365–90.
12. Chao J, et al. Tissue kallikrein in cardiovascular, cerebrovascular and renal diseases and skin wound healing. Biol Chem. 2010;391(4):345–55.
13. Fischer J, Meyer-Hoffert U. Regulation of kallikrein-related peptidases in the skin from physiology to diseases to therapeutic options. Thromb Haemost. 2013;110(3):442–9.
14. Sotiropoulou G, Pampalakis G. Kallikrein-related peptidases: bridges between immune functions and extracellular matrix degradation. Biol Chem. 2010;391(4):321–31.
15. Yousef GM, Diamandis EP. Expanded human tissue kallikrein family novel panel of cancer biomarkers. Tumour Biol. 2002;23(3):185–92.
16. Diamandis EP, Yousef GM, Luo LY, Magklara A, Obiezu CV. The human kallikrein gene family—implications in carcinogenesis. Trends Endocrinol Metab. 2000;11:54–60.
17. Yousef GM, Diamandis EP. The new human tissue kallikrein gene family: Structure, function and association to disease. Endocr Rev. 2001;22:184–204.
18. James GK, Pudek M, Berean KW, Diamandis EP, Archibald BL. Salivary duct carcinoma secreting prostate-specific antigen. Am J Clin Pathol. 1996;106:242–7.
19. Diamandis EP, Yousef GM. Human tissue kallikreins: a family of new cancer biomarkers. Clin Chem. 2002;48:1198–205.
20. Diamandis EP, Yousef GM. Human tissue kallikrein gene family: a rich source of novel disease biomarkers. Expert Rev Mol Diagn. 2001;1:182–90.
21. Obiezu C, Diamandis E. Human tissue kallikrein family: applications in cancer. Cancer Lett. 2005;224:1–22.
22. Ellis GL, Auclair PL, Gnepp DR. Surgical pathology of the salivary glands. Philadelphia: W.B. Saunders Company; 1991.
23. Davies L, Welch HG. Epidemiology of head and neck cancer in the United States. Otolaryngol Head Neck Surg. 2006;135:451–7.
24. Aro K, Leivo I, Makitie AA. Management and outcome of patients with mucoepidermoid carcinoma of major salivary gland origin: a single institution's 30-year experience. Laryngoscope 2008;118:258–62.
25. Borgono CA, Diamandis EP. The emerging roles of human tissue kallikreins in cancer. Nat Rev Cancer. 2004;4:876–90.
26. Darling MR, et al. Human kallikrein 6 expression in salivary gland tumors. J Histochem Cytochem. 2006;54:337–42.
27. Hashem NN, et al. Kallikrein-related peptidase 7 in salivary gland tumours: immunohistochemical expression profile. Can J Pathol. 2011;3(3):12–9.
28. Darling MR, et al. Human kallikrein 8 expression in salivary gland tumors. Head Neck Pathol. 2008;2:169–74.
29. Darling MR, et al. Kallikrein-related peptidase 10 expression in salivary gland tissues and tumours. Int J Biol Mark. 2012;27(4):e381–8.
30. Petraki CD, Karavana VN, Diamandis EP. Human tissues kallikrein 13 expression in normal tissues: an immunohistochemical study. J Histochem Cytochem. 2003;51:493–501.
31. Darling MR, Jackson-Boeters L, Daley TD, Diamandis EP. Human kallikrein 13 expression in salivary gland tumors. Int J Biol Mark. 2006;21(2):106–10.
32. Hashem NN, et al. Human kallikrein 14 (KLK14) expression in salivary gland tumors. Int J Biol Mark. 2010;25:32–7.
33. Darling MR, et al. Human kallikrein 3 (prostate-specific antigen) and human kallikrein 5 expression in salivary gland tumors. Int J Biol Mark. 2006;21(4):201–5.
34. Barnes L, Eveson J, Reichart P, Sidransky D. World Health Organization classification of tumours. Pathology and genetics of head and neck tumours. Lyon: International Agency for Research on Cancer (IARC) Press; 2005.
35. Culling CFA. Handbook of histopathological and histochemical techniques. 3rd ed. Oxford: Butterworth-Heinemann; 1974.
36. Shaw JL, Diamandis EP. Distribution of 15 human kallikreins in tissues and biological fluids. Clin Chem. 2007;53(8):1423–32.
37. Eissa A, Diamandis EP. Human tissue kallikreins as promiscuous modulators of homeostatic skin barrier functions. Biol Chem. 2008;389:669–80.
38. Emami N, Diamandis EP. New insights into the functional mechanisms and clinical applications of the kallikrein-related peptidase family. Mol Oncol. 2007;1:269–87.
39. Borgono CA, Michael IP, Diamandis EP. Human tissue kallikreins: physiologic roles and applications in cancer. Mol Cancer Res. 2004;2:257–80.
40. Sotiropoulou G, Pampalakis G, Diamandis EP. Functional roles of human kallikrein-related peptidases. J Biol Chem. 2009;284:32989–94.
41. Meyer-Hoffert U, Wu Z, Kantyka T, et al. Isolation of SPINK6 in human skin selective inhibitor of kallikrein-related peptidases. J Biol Chem. 2010;285(42):32174–81.
42. Bhoola KD, et al. Bioregulation of kinins: kallikreins, kininogens, and kininases. Pharmacol Rev. 1992;44:1–80.
43. Madeddu P, Emanueli C, El-Dahr S. Mechanisms of disease: the tissue kallikrein-kinin system in hypertension and vascular remodeling. Nat Clin Pract Nephrol. 2007;3:208–21.
44. Yayama K, et al. Tissue kallikrein is synthesized and secreted by human vascular endothelial cells. Biochim Biophys Acta. 2003;1593:231–8.
45. Dedio J, et al. Tissue kallikrein KLK1 is expressed de novo in endothelial cells and mediates relaxation of human umbilical veins. Biol Chem. 2001;382:1483–90.
46. Li XS, He XL. Kallikrein 12 downregulation reduces AGS gastric cancer cell proliferation and migration. Genet Mol Res. 2016;15(3):gmr.15038452.
47. Kapadia C, Yousef GM, Mellati AA, et al. Complex formation between human kallikrein 13 and serum protease inhibitors. Clin Chim Acta. 2004;339:157–67.
48. Kantyka T, Fischer J, Wu ZH, et al. Inhibition of kallikrein-related peptidases by the serine protease inhibitor of Kazal-type 6. Peptides 2011;32(6):1187–1192.
49. Ishige S, Kasamatsu A, Ogoshi K, et al. Decreased expression of kalllikrein-related peptidase 13: possible contribution to metastasis of human oral cancer. Mol Carcinogen. 2014;53(7):557–65.
50. Kapadia C, Ghosh MC, Grass L, Diamandis EP. Human kallikrein 13 involvement in extracellular matrix degradation. Biochem Biophys Res Commun. 2004;323:1084–90.
51. Rosai J, Ackerman LV. Rosai and Ackerman's surgical pathology. 10th ed. Edinburgh: Mosby; 2011.
52. Vercelli-Retta J, Almeida E, Ardao G, et al. Capsular pseudoinvasion after fine-needle aspiration of follicular adenomas of the thyroid. Diagn Cytopathol. 1997;17(4):295–7.
53. van Krieken JHJM. Prostate marker immunoreactivity in salivary gland neoplasms. Am J Surg Pathol. 1993;17(4):410–4.